J Electr Eng Technol.2015; 10(3): 786-794
http://dx.doi.org/10.5370/JEET.2015.10.3.786

ISSN(Print) 1975-0102
ISSN(Online) 2093-7423

Complementary Power Control of the Bipolar-type Low Voltage DC Distribution System

Gilsung Byeon†, Chul-Sang Hwang*, Jin-Hong Jeon*, Seul-Ki Kim*, Jong-Yul Kim*, Kisuk Kim, Bokyung Ko** and Eung-Sang Kim***

Abstract – In this paper, a new power control strategy for the bipolar-type low voltage direct current (LVDC) distribution system is being proposed. The dc distribution system is considered as an innovative system according to the increase of dc loads and dc output type distribution energy resources (DERs) such as photovoltaic (PV) systems and energy storage systems (ESS). Since the dc distribution system has many advantages such as feasible connection of DERs, reduction of conversion losses between dc output sources and loads, no reactive power issues, it is very suitable solution for new type buildings and residences interfaced with DERs and ESSs. In the bipolar-type, if it has each grid-interfaced converter, both sides (upper, lower-side) can be operated individually or collectively. A complementary power control strategy using two ESSs in both sides for effective and reliable operation is proposed in this paper. Detailed power control methods of the host controller and local controllers are described. To verify the performances of the proposed control strategy, simulation analysis using PSCAD/EMTDC is being performed where the results show that the proposed strategy provides efficient operations and can be applied to the bipolar-type dc distribution system.

Keywords: DC distribution system, DC microgrid, DC power control, Energy storage system, Bipolar type, PSCAD/EMTDC

1. Introduction

Because of a limited amount of fossil fuel and environmental pollution, efficiency enhancement and low carbon emissions have become an important issue in the field of power systems. To reduce the emission of greenhouse gases is achievable through the decrease of the various losses associated with generation, transmission, distribution and consumption of electrical power. In power systems, renewable energy resources (RES), energy storage systems (ESS) and electrical vehicles (EV) are considered as good alternatives to energy problems. The RES, ESS, and EV generate dc voltage and are connected to the dc bus. Therefore these components have to be interfaced with DC systems which are more efficient than AC systems. Furthermore, the increase of dc loads such as computers and electric lighting fixtures accelerate the introduction of dc systems. Recent statistical data suggests that the market related to dc systems is growing continuously, especially in village units [1]. Since 1990s, the dc power system analysis has been performed to set up the detailed aspects and apply to real sites. The dc power system analysis and modeling were studied in [2]. The challenges associated with the dc distribution system were addressed in [3]. The hybrid system which consists of PV, WT, and ESS and utilizes the common dc bus is introduced in [4]. The bipolar-type LVDC microgrid control scheme is introduced in [5]. From the viewpoint of the ESS applications and power control strategies, the ESS is implemented to improve energy efficiency of RESs such as PV in [6]. In [7] a composite ESS that contains both ultracapacitor and battery and control strategies in a microgrid is proposed. Various operation modes using a grid-connected converter and an energy storage device for a dc microgrid are described in [8]. The dc central supervisory controller with enabled communication interfaces is introduced in [9]. In [10], a dc system management scheme using EVs as the ESS for electric charge saving is described. One line-cycle regulation approach and one-sixth line-cycle regulation approach to control the dc bus voltage is introduced in [11]. Based on modifying the virtual resistances, droop control technologies are described in [12]. The fuzzy control method for PV-ESS system in dc microgrid is proposed in [13]. A cooperative droop control is introduced in [14]. This method is robust to disturbances in dc microgrid.

In many papers, in-depth studies on the transient control and stabilization system with ESSs have been conducted and various energy management schemes have been developed. In this paper, a complementary power control strategy using ESSs for effective and reliable operation is proposed. According to the grid connection, the bipolar-type LVDC system operation mode is divided into three

† Corresponding Author: Korea Electrotechnology Research Institute (KERI), Korea. (gsbyeon@keri.re.kr)
* KERI, Korea. (hcs1006@keri.re.kr, jhjeon@keri.re.kr, blksheep@keri.re.kr, jykim@keri.re.kr, eskim@keri.re.kr)
** School of Electrical Engineering, Korea University, Korea. (kks1213@korea.ac.kr, ok66551st@korea.ac.kr)
Received: October 7, 2014; Accepted: November 17, 2014

modes; both sides (upper and lower) are grid-connected (BGC), one is grid-connected and another is islanded (GC-IS), both sides are islanded (BIS). To make the best use of characteristics of the bipolar-type configuration, the host controller changes modes and locations of two ESSs. To verify the proposed control strategy, simulation tests are performed and discussed. This paper is organized as follows. Section II describes the bipolar-type LVDC distribution system configuration and controllers of individual components in detail. Section III represents the proposed complementary power control strategy to maximize the utility of ESSs. The results of the simulation tests and analysis studies are described and discussed in Section IV. Some comments about future works and conclusions are presented in Section V.

2. DC Distribution System Configuration

Generally, the LVDC distribution system is divided into unipolar and bipolar [15, 16]. Because of small capacity compared to the bipolar-type with the same voltage level (i.e. 750V and ±750 V), providing only one voltage level, the bipolar system is regarded more suitable for LVDC distribution system than unipolar in several papers and demonstration sites [5, 13, 16]. Since 2009, the IEC SMB SG4 aligns and coordinates activities in many areas where LVDC is used such as data centers, commercial buildings, and EV applications. They set the limit of low voltage as 1500V. The basic circuit of the bipolar-type LVDC distribution system is represented in Fig. 1. This system consists of a wind turbine generator (WT), a PV system, ESSs, a diesel generator, two common dc buses, power converters for conditioning the power associated with renewable resources and ESSs, distribution cables, and two grid-interfaced converters. Because of two grid-interfaced converters, the upper and lower side systems can be operated individually. If a certain energy source or load is connected to the 1,500V dc (±750 V dc) bus, two systems are connected and influence each other. The PV system is connected to the dc bus using a step-up dc-dc converter. This converter boosts the PV array voltage to the high voltage level of the dc bus. The WT system is consists of a turbine, a generator, and an ac-dc converter. This converter regulates active power to the dc bus depending on the variable wind speed. The ESS is composed of the battery stack and a bi-directional dc-dc converter. This converter is operated in active power control mode and voltage control mode. The state of charge (SOC) of battery stack is a factor for mode changes and is monitored in real-time. The diesel generator is connected to the dc bus using an ac-dc converter. This source is for emergency such as islanded. Its converter controls active power or dc voltage. The entire control system is divided into local controllers and a host controller. The maximum power point tracking (MPPT), current control, and electronics switching techniques are included in local controllers. The operation mode changes, power and voltage reference signal transfer to local controllers are main roles of the host controller. The host controller is the combination of a system-operation software, and communication system with local controllers. The host controller monitors states of the entire energy resources and electrical connections.

3. Complementary Power Control Strategy and Local Controllers

3.1 Host controller

The main control strategy of the host controller is presented in Fig. 2. There are three operation modes. Both sides are grid-connected (BGC), one is grid-connected and another is islanded (GC-IS), and both sides are islanded (BIS). The host controller monitors power flow and electrical connections. If a specific device is disabled or a line fault occurs, the host controller changes the operation mode among those three modes. The proposed control strategy can be applied to GC-IS and BIS modes. According to the grid connection and SOCs, ESSs are moved between the upper and lower sides. The detailed description of three operation modes is as follows

1) **BGC Mode** : In this mode, both upper and lower sides in LVDC system are connected to the grid. Two grid-interfaced inverters are operated in voltage control mode. The PV array and wind turbine generate the maximum power using the MPPT algorithm. All ESSs

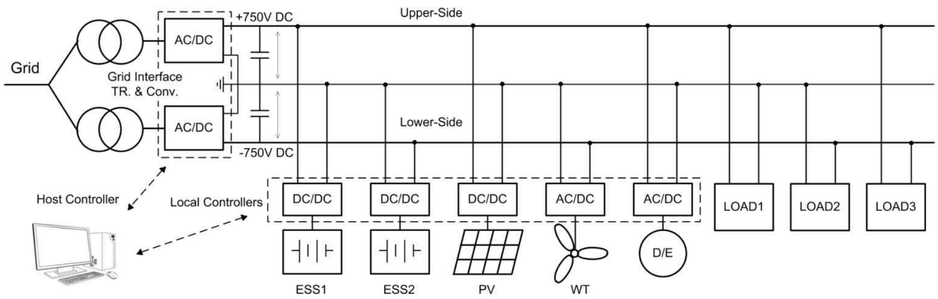

Fig. 1 Concept of a bipolar-type LVDC distribution system

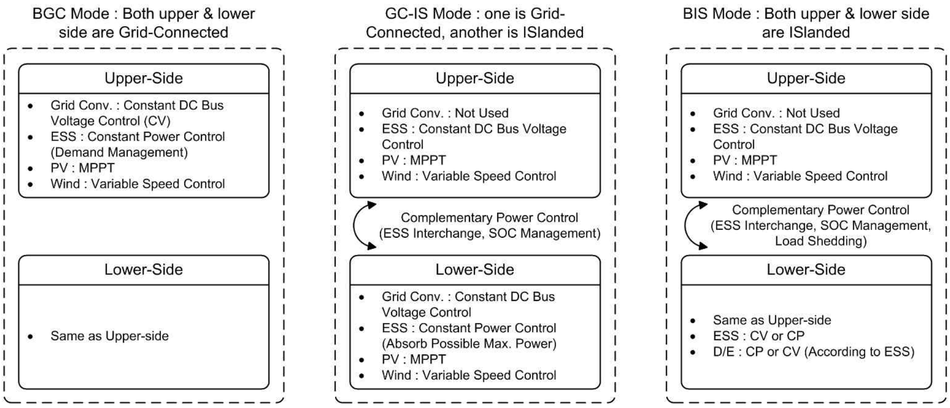

Fig. 2. Complementary power control strategy in three operation modes

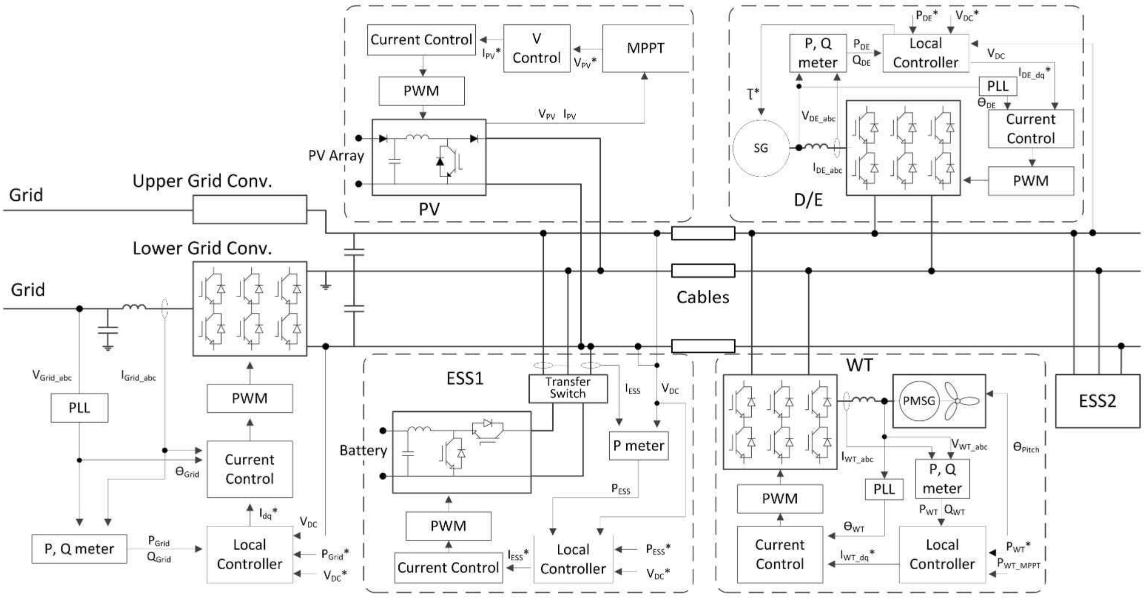

Fig. 3 Configuration and control blocks of local controllers

are operated in power control mode. If the time of use (TOU) rates exists, two ESSs are utilized to reduce electric rates as demand management (DM). If the incoming power from the grid is provided continuously and large capacity grid-interfaced converters are installed, all loads can be supplied active power even though all DERs in LVDC system have broken down.

2) **GC-IS Mode**: In this mode, one of two sides is not connected to the grid owing to a grid-interfaced converter or transformer failure. Therefore, one is operated in islanded mode, and another is operated in grid-connected mode. In islanded system, the PV and wind turbine generate maximum power and the ESS is operated in voltage control mode. If the electrical load is larger than the sum of the power output of the PV and wind turbine in islanded system, the SOC of ESS decreases continuously. In grid-connected system, the ESS is operated in power control mode. The host controller delivers the charging power reference signal to the ESS controller in GC mode. Most importantly, the charging rate of the ESS in GC mode is larger than the discharging rate of the ESS in IS mode. If the SOC of ESS in IS mode reaches the lower limit, the host controller interchanges the ESS in IS mode with the ESS in GC mode. The replaced ESS is connected and charged in GC side.

3) **BIS Mode** : In this mode, both sides are not connected to the grid because all grid-interfaced converters are disabled or a grid fault occurs. Two systems are operated in IS mode. If the diesel generator which can be operated in CV CP mode, it is the role of the grid in GC-IS mode temporarily. In the side which the DE exists, the ESS is charged moderately against the variable power output of RESs. When the electrical load is larger than the sum of the RES's power output and stored power of ESSs, the host controller performs load shedding and remains the minimum load.

3.2 PV controller

The PV array voltage depends on irradiation and surface temperature. To produce the maximum power output under a given condition, various maximum power point tracking techniques have been proposed [17, 18]. Among them, the incremental conductance technique is implemented in this paper. In all modes, the PV system is operated in the MPPT point. Detailed mathematical expression and flowchart of the PV controller are described in [4, 19].

3.3 WT controller

The Wind turbine is a device that converts kinetic energy from the wind into electrical power. Generally, the wind turbine is operated to obtain the maximum power from varying wind speeds [20]. If the operator wants to decrease the power output under a given wind speed, the control system adjusts the blade pitch to keep the rotor speed within operating limits as the wind speed changes. In Fig. 3, Control blocks of the WT system are represented. The WT system is operated to produce the maximum power in this paper. Detailed mathematical expression and flowchart of the WT controller are described in [4, 21, 22].

3.4 DE controller

In Fig. 3, control blocks of the diesel generator system is represented. Control of the diesel generator is similar to that of the WT system. However, power and voltage control blocks are added to control dc bus voltage. Therefore, the local controller sets the torque and current reference together. In the proposed control strategy, the diesel generator system is only operated in BIS mode.

3.5 ESS controller

The roles of ESSs are to generate or absorbs active power (CP), and regulate dc bus voltage (CV). As mentioned in Chapter 3.1, two ESSs are operated in CP mode and participate in DM (BGC mode). In GC-IS mode, the ESS in islanded mode is operated in CV mode. In BIS mode, the ESS in the system without the D/E is operated in CV mode. Fig. 4 shows the power and voltage controller of the ESS converter. By commands from the host controller, the operation mode is changed. In Fig. 3, all control blocks of the ESS are represented. Two ESSs are connected to the

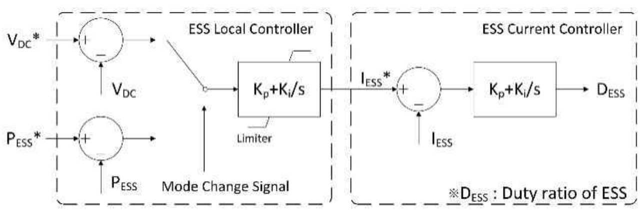

Fig. 4 Power and Voltage Controller of the ESS

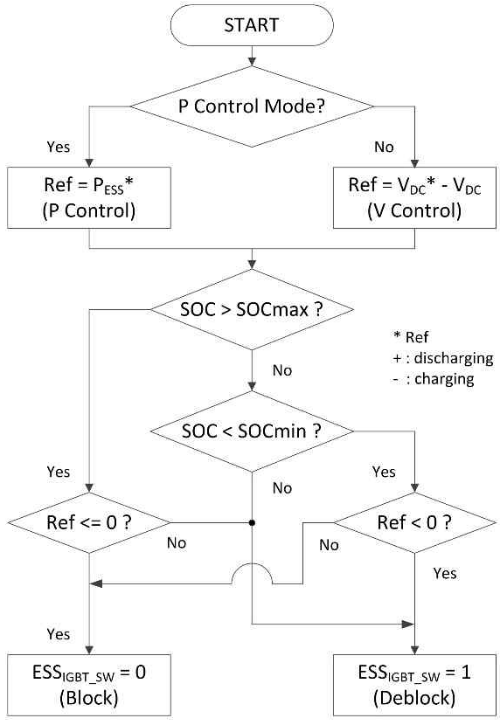

Fig. 5. Flowchart of the SOC limiter

upper and lower sides using switches and moved from one side to another side according to the host controller command. The flowchart of the SOC limiter is represented in Fig. 5. The SOC limiter prevents overcharge and overdischarge. If the SOC reaches the upper and lower limit, the SOC limiter sends block signals to the IGBT gate driver. The SOC limiter turns the gate driver on according to the direction of power flow.

4. Case Study

Focused on dynamic behaviors, three simulation cases were performed to validate the proposed control strategy. All cases are simulated using PSCAD/EMTDC software. Detailed mathematical descriptions and models are available in [4, 19, 21]. The system configuration and parameters are represented in Fig. 3 and appendix.

4.1 BGC mode

Fig. 6 presents dynamic responses of upper side components according to the electricity price time and SOC of ESS. The negative sign of grid power means the amount of incoming power. In BGC mode, if TOU rates exist, two ESSs participated in DM at each side. In the light and medium price time (until 8.0s), the ESS absorbs oversupply of RESs and does not discharge. In the heavy price time, the ESS discharges to provide active power instead of the grid. This scheme has an effect on electric charge saving. Detailed description about DM using the

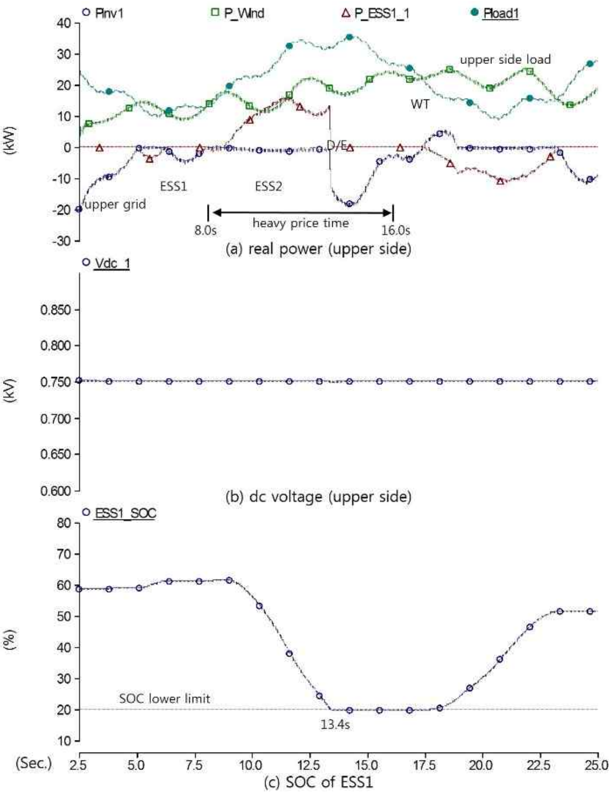

Fig. 6. Simulation results of the upper side in BGC mode: (a) active power; (b) dc voltage profile; (c) SOC of ESS1

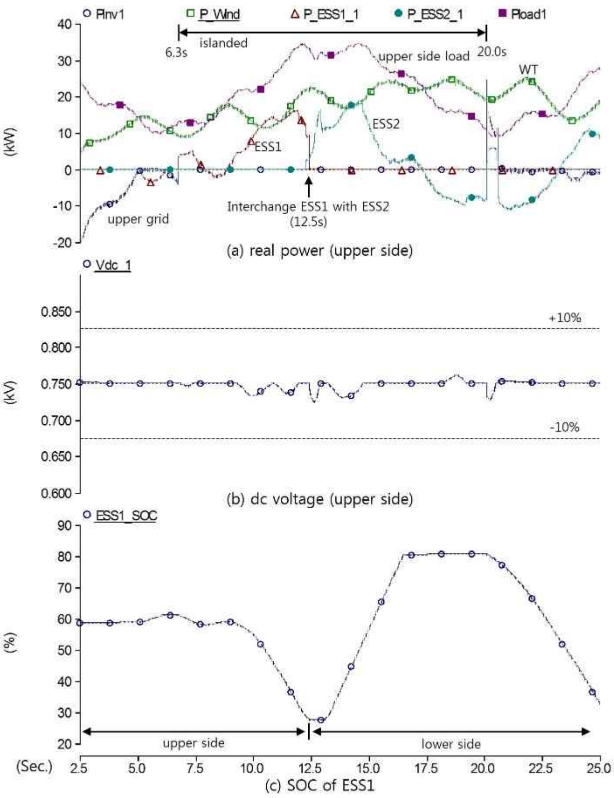

Fig. 7. Simulation results of the upper side in GC-IS mode. (a) active power. (b) dc voltage profile. (c) SOC of ESS1

ESS is represented in [23, 24]. When the ESS1 reaches the lower limit (13.4s), the ESS1 stops discharging and the grid power is injected. In BGC mode, dc bus voltages in both sides are seldom fluctuated because they are controlled by grid-interfaced converters.

4.2 GC-IS mode

The complementary power control performances of the ESSs in GC-IS mode were simulated. Unlike GC mode, the most important role of the ESS in IS mode is to control dc bus voltage and provide the power to loads stably. Fig. 7, 8 present dynamic responses of the upper and lower side components according to the grid connection and the SOC of ESSs. Active power curves of upper side components are presented in Fig. 7(a). Until 6.3s, the upper and lower side systems are operated in GC mode. Because the electricity price is cheap at this time, ESSs are operated to minimize the discharging power. At 6.3s, the injection power to the upper side is interrupted (Pinv1 in Fig. 7 (a) becomes zero at 6.3s). As soon as the host controller detects this interrupt, it sends the mode change command to local controllers in the upper and lower sides. The ESS in the upper side (ESS1) changes the power control mode to the voltage control mode immediately. And the ESS in the lower (ESS2) side keeps the charging mode. The charging power of ESS2 must be larger than the discharging power of ESS1. After 6.3s, ESS1 control dc voltage in the upper side and its SOC decreases continuously owing to large electrical loads (Fig. 7 (c)).

Because of intended charging, the SOC of ESS2 reaches its upper limit and ESS2 stops charging. When the SOC of ESS1 reaches the warning limit (30% in this simulation), ESS2 is moved from the lower side to the upper side and operated in voltage control mode (at 12.5s). Then ESS1 stops controlling voltage and is moved from the upper side to lower side. Because the upper side is still islanded, ESS1 starts intended charging for next interchange (from 13s). Until 17.5s, the SOC of ESS2 decreases continuously. Then it rebounds owing to the wind power increase and load decrease. At 20.0s, the upper side is ready for the grid connection. The host controller permits the reconnection and the grid controls the upper side dc voltage. Then the upper and lower sides are operated again in GC mode. Because the electricity price is high after 20.0s, ESSs are operated to minimize the injection power from the grid. The dc voltage in the upper side fluctuates owing to mode changes (GC→IS→GC), ESS interchange, sudden load variation. The maximum fluctuation rate measures about 3.1%. Considering that there are not any guidelines and standards related to the dc voltage fluctuation rate in islanded mode and the ac low voltage fluctuation rate in grid-connected mode is within ±10%, this result is regarded as reasonable.

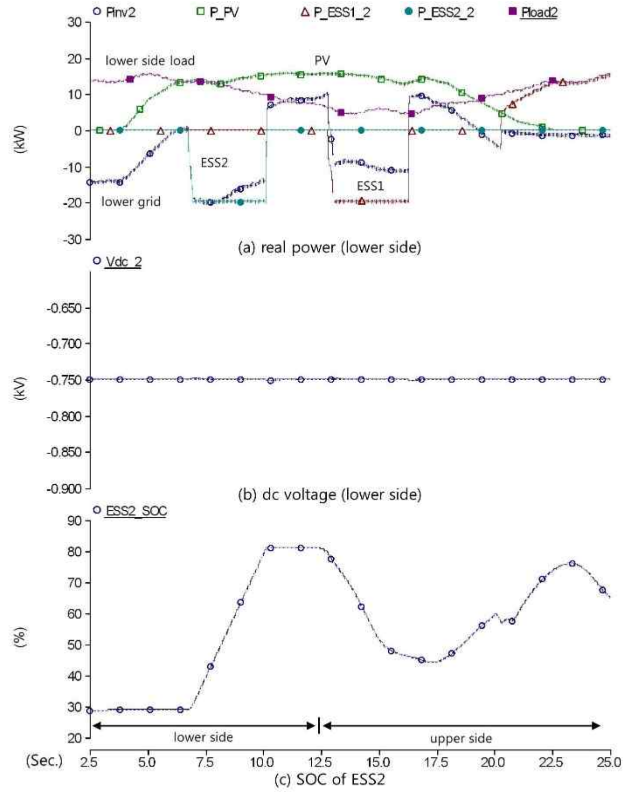

Fig. 8. Simulation results of the lower side in GC-IS mode. (a) active power. (b) dc voltage profile. (c) SOC of ESS2

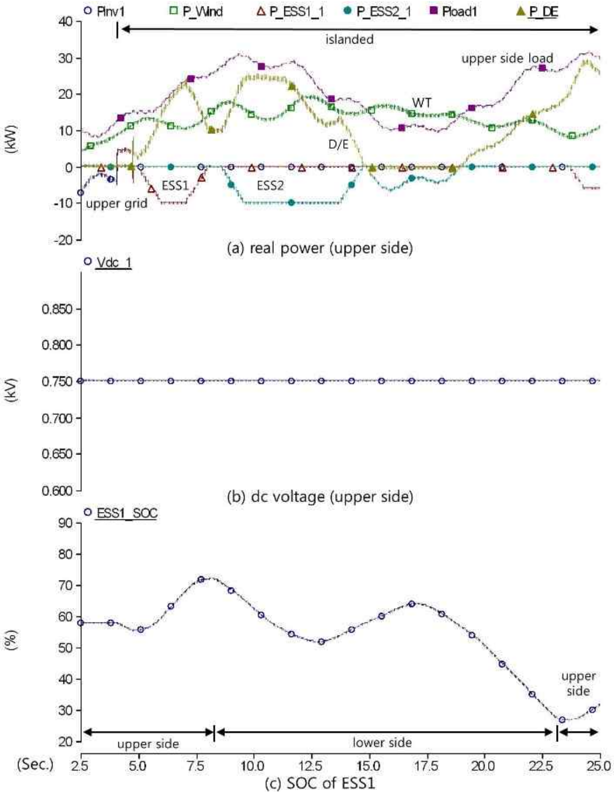

Fig. 9. Simulation results of the upper side in BIS mode: (a) active power; (b) dc voltage profile; (c) SOC of ESS1

4.3 BIS mode

The complementary power control performances of the ESSs in BIS mode were simulated. Fig. 9, 10 present dynamic responses of the upper and lower side components. Active power curves of the upper and lower side components are presented in Fig. 9 and 10 (a). Until 4.0s, the upper and lower side systems are operated in GC mode. At 4.0s, the injection power to both sides is interrupted (Pinv1 in Fig. 9 (a) and Pinv2 in Fig 10. (a) become zero at 4.0s). ESSs in both sides change power control mode to voltage control mode immediately. The diesel generator in the upper side is turned on and increases power output. Because the ESS has fast dynamic characteristics, it controls the dc voltage for a short time and the diesel generator receives a role. Then the ESS1 starts intended charging. The diesel generator cannot increase power output rapidly compared with the injection power from the grid. Therefore, intended charging rate is lower than that of GC-IS mode. In the lower side, the SOC of ESS2 decreases and reaches the warning limit (below 30%), ESS1 is moved from the upper side to lower side and operated in voltage control mode (at 8.2s). Then ESS2 stops controlling the voltage and is moved from the lower side to upper side. ESS2 starts intended charging for next interchange and absorbs the oversupply from the WT system. If power output forecasts and estimations of RESs

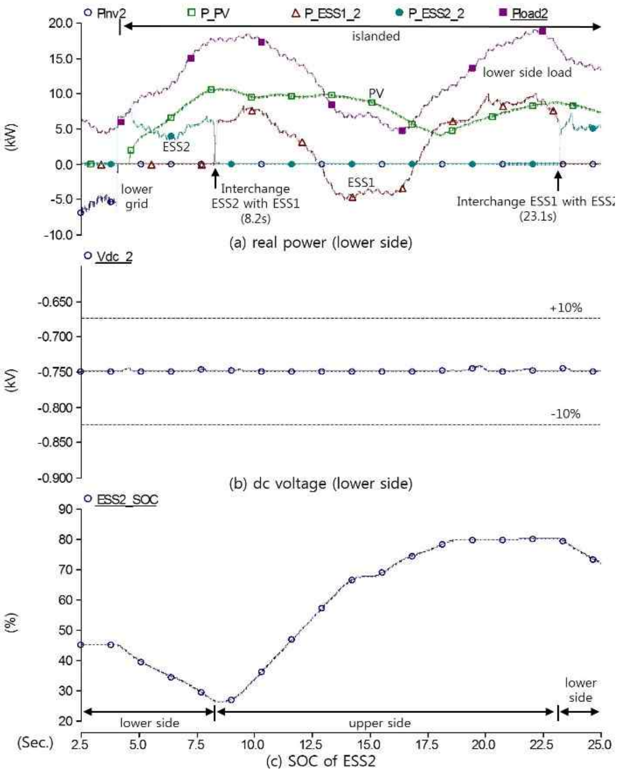

Fig. 10. Simulation results of the lower side in GC-IS mode: (a) active power; (b) dc voltage profile; (c) SOC of ESS2

are performed beforehand, intended charging amount can be controlled more precisely. The ESS1 controls the dc voltage of the lower side from 8.2s to 23.1s and its SOC fluctuates continuously. At 23.1s the SOC of ESS1 reaches the warning limit, ESS2 is moved from the upper side to lower side and operated in voltage control mode. In this simulation, both side systems can be operated in relatively stable state (power supply and voltage profile) using a diesel generator and complementary power control scheme. However, if the load is larger than the amount of electricity generated (D/E, WT, PV and ESSs), the load shedding must be considered.

5. Conclusion

In this paper, a complementary control strategy for the bipolar-type LVDC distribution system using ESSs has been proposed. Three operation modes to maximize the effect of ESSs have been described. This complementary ESS control strategy improves the electrical power supply capacity to all loads (±750V and 1.5kVdc) in GC-IS, BIS mode. The SOC management strategy makes simulation studies more realistic. The dynamic modeling and simulation studies of the bipolar-type LVDC system under the proposed control strategy were carried out using PSCAD/EMTDC. The host controller and local controllers were implemented and tested. A comprehensive result through simulation tests has shown that the proposed control strategy which enabled quantitative and qualitative analysis before a real hardware demonstration. In future works, an experimental study will be performed using real components (PV, WT, Li-ion batteries, etc..) and the real-time digital simulator (RTDS). Especially, novel interchange techniques of real ESSs will be studied to prevent severe transient and assure stability.

Appendix

1) Grid-interfaced converters (upper and lower sides)
   - Conv. type : 3phase PWM ac/dc converter
   - Power rating : 50kW
   - I/O voltage : 380Vac / 750Vdc
   - TR I/O voltage : 22.9kVac / 380Vac
   - Control mode : CP, CV
2) PV system (lower side)
   - Conv. type : boost dc/dc converter
   - Power rating : 20kW
   - Control mode : MPPT
3) WT system (upper side)
   - Conv. type : 3phase PWM ac/dc converter
   - Gen. type : PMSG
   - Power rating : 30kW
   - Control mode : MPPT, pitch control
4) DE system (upper side)
   - Conv. type : 3phase PWM ac/dc converter
   - Gen. type : PMSG
   - Power rating : 30kW
   - Control mode : CP, CV
5) ESSs (upper and lower sides)
   - Conv. type : bidirectional dc/dc converter
   - Power rating : 20kW
   - Control mode : CP, CV, SOC control
6) Loads
   - DC load1 (upper side) : 750Vdc, 0~35kW
   - DC load2 (lower side) : 750Vdc, 0~20kW
   - DC load3 (both sides) : 1.5kVdc, 3.75kW
7) Cables
   - TFR-CV 35mm2, 0.5km
   - L : 0.0023661H/km, R : 0.669Ω/km

References

[1] Navigant Research, "Direct Current Distribution Networks; Remote and Grid-Tied Systems for Data Center Microgrids, Telecom/Village Power, Commercial Buildings, and Military Applications: Global Market Analysis and Forecasts", 2013.

[2] K. Fleischer and R. S. Munnings, "Power systems analysis for direct current (DC) distribution systems," IEEE Trans. Ind. Appl., vol. 32, no. 5, pp. 982-989, Sep./Oct. 1996.

[3] M. Baran and N. R. Mahajan, "DC distribution for industrial systems: Opportunities and challenges," IEEE Trans. Ind. Appl., vol. 39, no. 6, pp. 1596-1601, Nov./Dec. 2003.

[4] S. K. Kim, J. H. Jeon, C. Cho, J. B. Ahn, and S. H. Kwon, "Dynamic Modeling and Control of a Grid-Connected Hybrid Generation System With Versatile Power Transfer," IEEE Trans. Ind. Electron., vol. 55, no. 4, pp. 1677-1688, Apr. 2008.

[5] H. Kakigano, Y. Miura, and T. Ise, "Low-voltage bipolar-type DC microgrid for super high quality distribution," IEEE Trans. Power Electron., vol. 25, no. 12, pp. 3066-3075, Dec. 2010.

[6] K. Sun, L. Zhang, Y. Xing, and J. Guerrero, "A distributed control strategy based on DC bus signaling for modular photovoltaic generation systems with battery energy storage," IEEE Trans. Power Electron., vol. 26, no. 10, pp. 3032-3045, Oct. 2011.

[7] H. Zhou, T. Bhattacharya, D. Tran, T. S. T. Siew, and A. M. Khambadkone, "Composite energy storage system involving battery and ultracapacitor with dynamic energy management in microgrid applications," IEEE Trans. Power Electron., vol. 26, no. 3, pp. 923-930, Mar. 2011.

[8] L. Xu and D. Chen, "Control and Operation of a DC Microgrid With Variable Generation and Energy Storage", IEEE Trans. Power Electron., vol. 26, no. 4, pp. 2513-2522, Oct. 2011.

[9] H. Valderrama-Blavi, J. M. Bosque, F. Guinjoan, L. Marroyo, and L. Martinez-Salamero, "Power adaptor device for domestic dc microgrids based on commercial mppt inverters," IEEE Trans. Ind. Electron., vol. 60, no. 3, pp. 1191-1203, Mar. 2013.

[10] G. Byeon, T. Yoon, S. Oh and G. Jang, "Energy Management Strategy of the DC Distribution System in Buildings Using the EV Service Model," IEEE Trans. Power Electron., vol. 28, no. 4, pp. 1544-1554, Sep. 2013.

[11] T. F. Wu, C. H. Chang, L. C. Lin, G. R. Yu and Y. R. Chang, "DC-Bus Voltage Control With a Three-Phase Bidirectional Inverter for DC Distribution Systems", IEEE Trans. Power Electron., vol. 28, no. 4, pp. 1890-1899, Apr. 2013.

[12] N. L. Diaz, T. Dragicevic, J. C. Vasqeuz and J. M. Guerrero, "Intelligent Distributed Generation and Storage Units for DC Microgrids — A New Concept on Cooperative Control Without Communications Beyond Droop Control," IEEE Trans. Smart Grid, vol. 5, no. 5, pp. 2476-2485, Sep. 2014.

[13] R. F. Bastos, C. R. Aguiar, A. F. Q. Goncalves and R. Q. Machado, "An Intelligent Control System Used to Improve Energy Production From Alternative Sources With DC/DC Integration," IEEE Trans. Smart Grid, vol. 5, no. 5, pp. 2486-2495, Sep. 2014.

[14] A. Maknouninejad, Z. Qu, L. Lewis and A. Davoudi, "Optimal, Nonlinear, and Distributed Designs of Droop Controls for DC Microgrids," IEEE Trans. Smart Grid, vol. 5, no. 5, pp. 2508-2516, Sep. 2014.

[15] A. Sannino, G. Postiglione, and M. H. J. Bollen, "Feasibility of a DC network for commercial facilities," IEEE Trans. Ind. Appl., vol. 39, no. 5, pp. 1499-1507, Sep./Oct. 2003.

[16] T. Kaipia, P. Salonen, J. Lassila, and J. Partanen, "Possibilities of the low voltage DC distribution systems," In Proc. of NORDAC 2006 Conf., Stockholm, Sweden, August 2006.

[17] H. Koizumi et al., "A novel microcontroller for grid-connected photovoltaic systems," IEEE Trans. Ind. Electron., vol. 53, no. 6, pp. 1889-1897, Dec. 2006.

[18] E. Roman et al., "Intelligent PV module for grid-connected PV systems," IEEE Trans. Ind. Electron., vol. 53, no. 4, pp. 1066-1073, Aug. 2006.

[19] M. Park and I.-K. Yu, "A novel real-time simulation technique of photovoltaic generation systems using RTDS," IEEE Trans. Energy Convers., vol. 19, no. 1, pp. 164-169, Mar. 2004.

[20] A. Miller, E. Muljadi, and D. Zinger, "A variable speed wind turbine power control," IEEE Trans. Energy Convers., vol. 12, no. 2, pp. 181-186, Jun. 1997.

[21] S.-K. Kim and E.-S. Kim, "PSCAD/EMTDC based modeling and analysis of a gearless variable speed wind turbine," IEEE Trans. Energy Convers., vol. 22, no. 2, pp. 421-430, Jun. 2007.

[22] G. Kim, J. Kim, S. Kim, E. Kim, J. Lee, M. Park and I. Yu, "Hardware-in-the-loop Simulation Method for a Wind Farm Controller Using Real Time Digital Simulator," Journal of Electrical Engineering and Technology, vol. 9, no. 5, pp. 1489-1494, Sep. 2014.

[23] K.-H. Cho, S.-K. Kim and E.-S. Kim, "Optimal capacity determination method of battery energy storage system for demand management of electricity customer," The Tran. of Korea Institute of Electrical Engineers, vol. 62, no. 1, pp. 21-28, 2013.

[24] M. Rastegar, M. F. Firuzabad and J. Choi. "Investigating the Impacts of Different Price-Based Demand Response Programs on Home Load Management," Journal of Electrical Engineering and Technology, vol. 9, no. 3, pp. 742-748, May. 2014.

Gilsung Byeon He received B.S and Ph.D degrees from the School of Electrical Engineering, Korea University in 2006 and 2012. Currently, he works as a senior researcher with the smart distribution research center, Korea Electrotechnology Research Institute (KERI).

Chul-Sang Hwang He received B.S and M.S degrees in department of electrical engineering from Changwon National University, and currently a Ph.D course student in the same University. He is working as assistance researcher with the smart distribution research center, KERI.

Jin-Hong Jeon He received his B.S. and M.S. from Sungkyunkwan University in 1995 and 1997, respectively, and his Ph.D. from Pusan National University, Korea, in 2012, in the department of electrical engineering. Currently, he works as a principal researcher with the smart distribution research center, KERI.

Seul-Ki Kim He received the B.S., M.S and Ph.D. degrees in electrical engineering from Korea University, Seoul, Korea, in 1998, 2000 and 2010 respectively. Currently, he works as a principal researcher with the smart distribution research center, KERI

Jong-Yul Kim He received his B.S. and M.S. and Ph.D. degrees in Electrical Engineering from Pusan National University, Korea in 1997, 1999, and 2011, respectively. Currently, he works as a senior researcher with the smart distribution research center, KERI.

Kisuk Kim He received a B.S. degree in electrical engineering from Soongsil University, Seoul, Korea in 2010 and an M.S. degree from Korea University, Seoul, Korea in 2013. He is currently pursuing a Ph.D. degree at Korea University.

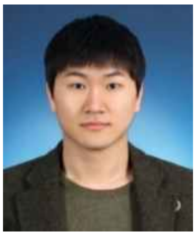

Bokyung Ko He received the B.S. and M.S. degrees in the school of electrical engineering from the Korea University, Seoul, South Korea in 2011 and 2013 respectively. He is currently pursuing his Ph.D. degree in electrical engineering from Korea University, Seoul, South Korea.

Eung-Sang Kim He received the B.S. degree in electrical engineering from Seoul National University of Technology and the M.S. and Ph.D. degree in electric engineering from Soong-Sil University. Currently, he is a principal researcher with the smart distribution research center, KERI.